Glycobiology, 2019, vol. 29, no. 1, 22–35
doi: 10.1093/glycob/cwy099
Advance Access Publication Date: 22 November 2018
Original Article

Cell Biology

Galectin-9 induces atypical ubiquitination leading to cell death in PC-3 prostate cancer cells

Aiko Itoh[2], Yasuhiro Nonaka[3], Takashi Ogawa[3], Takanori Nakamura[3], and Nozomu Nishi[2,1]

[2]Division of Research Instrument and Equipment, Life Science Research Center, Kagawa 761-0793, Japan and [3]Department of Endocrinology, Faculty of Medicine, Kagawa University, 1750-1 Ikenobe, Miki-cho, Kita-gun, Kagawa 761-0793, Japan

[1]To whom correspondence should be addressed: Tel: +81-87-891-2258; Fax: +81-87-891-2260; e-mail: nnishi@med.kagawa-u.ac.jp

Received 19 June 2018; Revised 24 August 2018; Editorial decision 22 October 2018; Accepted 24 October 2018

Abstract

Galectin-9 is the most potent inducer of cell death in lymphomas and other malignant cell types among the members of the galectin family. We investigated the mechanism of galectin-9-induced cell death in PC-3 prostate cancer cells in comparison with in Jurkat T cells. Galectin-9 induced apoptotic cell death in Jurkat cells, as typically revealed by DNA ladder formation. On the other hand, DNA ladder formation and other features of apoptosis were not apparent in PC-3 cells undergoing galectin-9-induced death. Exogenous galectin-9 was endocytosed and destined to the lysosomal compartment in PC-3 cells. The internalized galectin-9 was resistant to detergent solubilization but was solubilized with lactose. Agents inhibiting actin filament dynamics abolished the internalization and cytocidal effect of galectin-9 in PC-3 but not Jurkat cells. Galectin-9 induced accumulation of ubiquitinated proteins, possibly heterogeneously ubiquitinated and/or monoubiquitinated proteins, in PC-3 cells. PYR-41, an inhibitor of the ubiquitin-activating E1 enzyme, suppressed the cytocidal effect of galectin-9. Although ubiquitination was upregulated also in Jurkat cells by galectin-9, PYR-41 was ineffective against galectin-9-induced cell death. Colocalization of ubiquitinated proteins and LAMP-1 was detectable in PC-3 cells treated with galectin-9. The ubiquitinated proteins were recovered in the insoluble fraction upon cell fractionation. In contrast, ubiquitinated proteins that accumulated after treatment with proteasome inhibitors did not co-localize with LAMP-1 and were mainly recovered in soluble fraction. The results suggest that atypical ubiquitination and accumulation of ubiquitinated proteins in lysosomes play a pivotal role in galectin-9-induced non-apoptotic death in PC-3 cells.

Key words: autophagy, endocytosis, alectin, lysosome, ubiquitination

Introduction

Galectins comprise a family of mammalian lectins defined by an evolutionary conserved carbohydrate recognition domain (CRD) with preferential affinity for lactosamine-type disaccharides. They are essentially intracellular cytosolic proteins lacking signal sequences. Identification of galectin-8 (Gal-8) as a danger receptor, which triggers intracellular antibacterial autophagy, is a typical example of intracellular roles of the galectin family (Thurston et al. 2012). Gal-3, another member of the family, also plays an essential role in selective autophagy in cooperation with TRIM16 (Chauhan et al. 2016). In spite of their cytosolic

nature, galectins have been assumed to be secreted via a non-classical pathway (Hughes 1999), and to act extracellularly in an autocrine/paracrine manner through interactions with cell surface glycoconjugates. There are currently about 10 members of the human galectin family, which can be classified into three subtypes based on their structures (Hirabayashi and Kasai 1993). The proto-type (Gal-1, -2, -7, -10, -13, and -14) and chimera-type (Gal-3) galectins have a single CRD, while the tandem-repeat-type galectins (Gal-4, -8, -9 and -12) have two CRDs with different binding specificities joined by a linker region.

Gal-9 is a unique member of the tandem-repeat-type subfamily with potent immune-modulating activity. Gal-9 is essentially an immune system suppressor: it promotes differentiation of regulatory T-cells (Tregs), and reduces T-helper 17 (Th17) and Th1 cells (Zhu et al. 2005; Seki et al. 2008), resulting in suppression of excessive immunity and inflammation. In accordance with the immune suppressing action, treatment with recombinant Gal-9 exhibited therapeutic efficacy in mouse autoimmune disease models including rheumatoid arthritis (Seki et al. 2007, 2008), experimental autoimmune encephalomyelitis (Zhu et al. 2005), and type I diabetes mellitus (Chou et al. 2009; Kanzaki et al. 2012). In addition, Gal-9 inhibits allograft rejection (He et al. 2009), and ameliorates graft versus host disease (Sakai et al. 2011) and allergic asthma (Niki et al. 2009). These therapeutic effects of Gal-9 have been demonstrated primarily by pharmacological studies, in which a genetically modified form of Gal-9 instead of the wild-type one was mainly used. The linker region of the tandem-repeat-type galectins is intrinsically disordered/unstructured and hence highly susceptible to a variety of proteases. For example, affinity purified G9M, a major isoform (splice variant) of wild-type Gal-9, was rapidly degraded by contaminating protease(s) upon storage under sterile conditions (Nishi et al. 2005). Dissociation of the two CRDs through proteolysis at the linker region leads to a drastic decrease in the biological activity of Gal-9, making it difficult to efficiently perform experiments, especially in vivo ones, using recombinant wild-type proteins. In order to overcome the protease sensitivity and low solubility of wild-type Gal-9, we developed genetically modified forms of Gal-9, G9Null (a stable form of Gal-9 with a partially truncated linker peptide) and ssG9 (a highly stable and soluble form of Gal-9 without a linker peptide) (Nishi et al. 2005; Itoh et al. 2013). Human lymphoma cell lines (MOLT-4 and Jurkat) and a prostatic cancer cell line (PC-3) were used to assess the effect of structural modifications on the cytocidal effect of Gal-9 in these studies. The mechanism of action of Gal-9 as to lymphoma cell lines has been extensively studied: Gal-9-induced apoptotic cell death via caspase-dependent or -independent pathways in the cell lines (Kashio et al. 2003; Lu et al. 2007). On the other hand, the mechanism underlying Gal-9-induced cell death in adherent cells including PC-3 cells is not fully understood and seems largely dependent on the cell type (Wiersma et al. 2015). In this study, we investigated Gal-9-induced cell death in PC-3 cells in comparison with in Jurkat cells regarding intracellular signaling, endocytic internalization of Gal-9, and endogenous protein degradation systems. This study serves to establish PC-3 cells as one of the standard cell lines for quality control of recombinant Gal-9 preparations in future therapeutic use.

Results

Gal-9 is a potent inducer of non-apoptotic cell death in PC-3 cells

Gal-9 (G9Null) is the most potent inducer of cell death among the members of the galectin family examined (Figure 1A). The viable

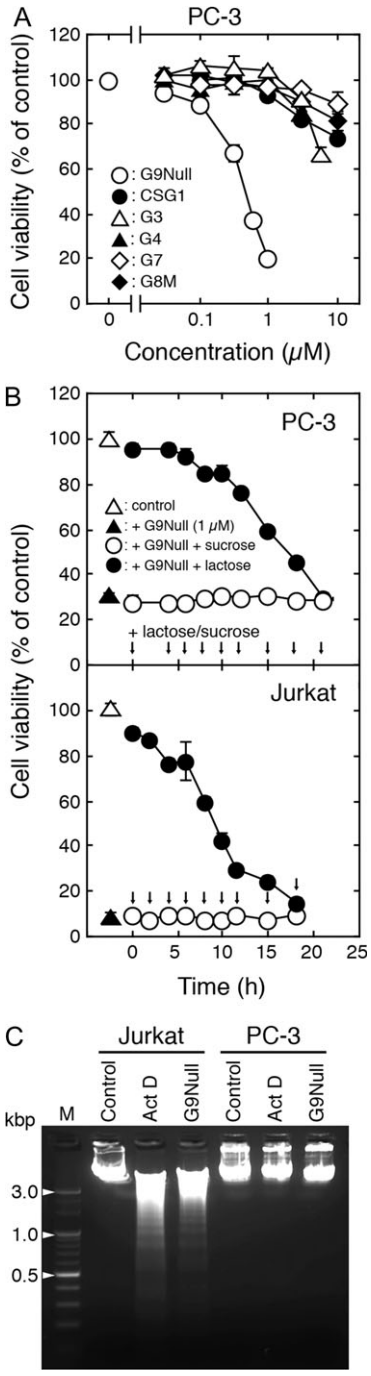

Fig. 1. Characteristics of Gal-9-induced cell death. (**A**) The cytocidal effects of Gal-9 and other members of the galectin family on PC-3 cells were determined by means of the WST-8 assay. Each assay was performed in triplicate. The results are presented as mean ± SD (*error bars*). (**B**) The effect of contact time with G9Null on the viability of PC-3 (upper panel) and Jurkat (lower panel) cells was assessed by means of the WST-8 assay. Lactose or sucrose was added to the culture medium to give a final concentration of 20 mM at the indicated times (*arrows*) after the addition of G9Null (1 μM). (**C**) DNA extracted from Jurkat and PC-3 cells was analyzed by agarose gel electrophoresis. Cells were treated with PBS (control), actinomycin D (2 μM), and G9Null (1 μM) for 24 h. *CSG1/G3/G4/G7*, CSGal-1/Gal-3/Gal-4/Gal-7; *G8M*, a major isoform (splice variant form) of Gal-8; *M*, DNA size markers; *ActD*, actinomycin D.

cell number decreased to about 67%, 37% and 20% of the control level on incubation with 0.3 μM, 0.6 μM and 1 μM of Gal-9, respectively, for 24 h under the conditions used. The time-dependent changes in cell viability and morphology of PC-3 cells induced by Gal-9 are shown in Supplementary Figure S1. CSGal-1 (a cysteine-less mutant of Gal-1), Gal-3, -4, -7, and -8 exhibited a negligible effect on PC-3 cell viability at 1 μM. The addition of lactose (an inhibitory disaccharide for Gal-9) to the culture medium after 10-h incubation with Gal-9 and subsequent 14-h culture (total culture time of 24 h) abolished most of the cytocidal effect on PC-3 cells, whereas sucrose, a non-inhibitory disaccharide, had no effect (Figure 1B, upper panel). The contact time needed for Gal-9 to induce a high level of cell death was longer than ~15 h. On the other hand, addition of lactose after 10-h incubation with Gal-9 resulted in a 60% decrease in the viable cell number of Jurkat cells (Figure 1B, lower panel). DNA ladder formation, a typical symptom of apoptotic cells, was detectable in Jurkat but not PC-3 cells undergoing Gal-9-induced death (Figure 1C). It seems difficult to induce the apoptotic process leading to DNA fragmentation in PC-3 cells because actinomycin D (2 μM) and other apoptosis inducers, i.e., staurosporine (1 μM), cycloheximide (10 μM) and etoposide (10 μM), also did not induce DNA fragmentation (data not shown). In accordance with the results, activation of caspase 3 was not detected in PC-3 cells upon treatment with Gal-9, and a pan-caspase inhibitor (Z-VAD-FMK) was ineffective in neutralizing the effect of Gal-9 (data not shown).

Activation of p38 mitogen-activated protein kinase (MAPK) and c-Jun N-terminal kinase (JNK) pathways is dispensable for Gal-9-induced death in PC-3 cells

It has been reported that Gal-9 exerts a cytocidal effect on multiple myeloma cell lines through the p38 MAPK and JNK pathways. Gal-9 upregulated phosphorylation of p38 MAPK and JNK in the cell lines, and inhibitors of the kinases, especially a p38 MAPK inhibitor (SB203580), almost completely suppressed the effect of Gal-9 in IM9 cells (Kobayashi et al. 2010). Phosphorylation of p38 MAPK and JNK was also markedly increased in PC-3 cells treated with Gal-9 (Figure 2A): the increases in the phosphorylated forms of p38 MAPK and JNK were evident 4–8 h and 1 h after the addition of

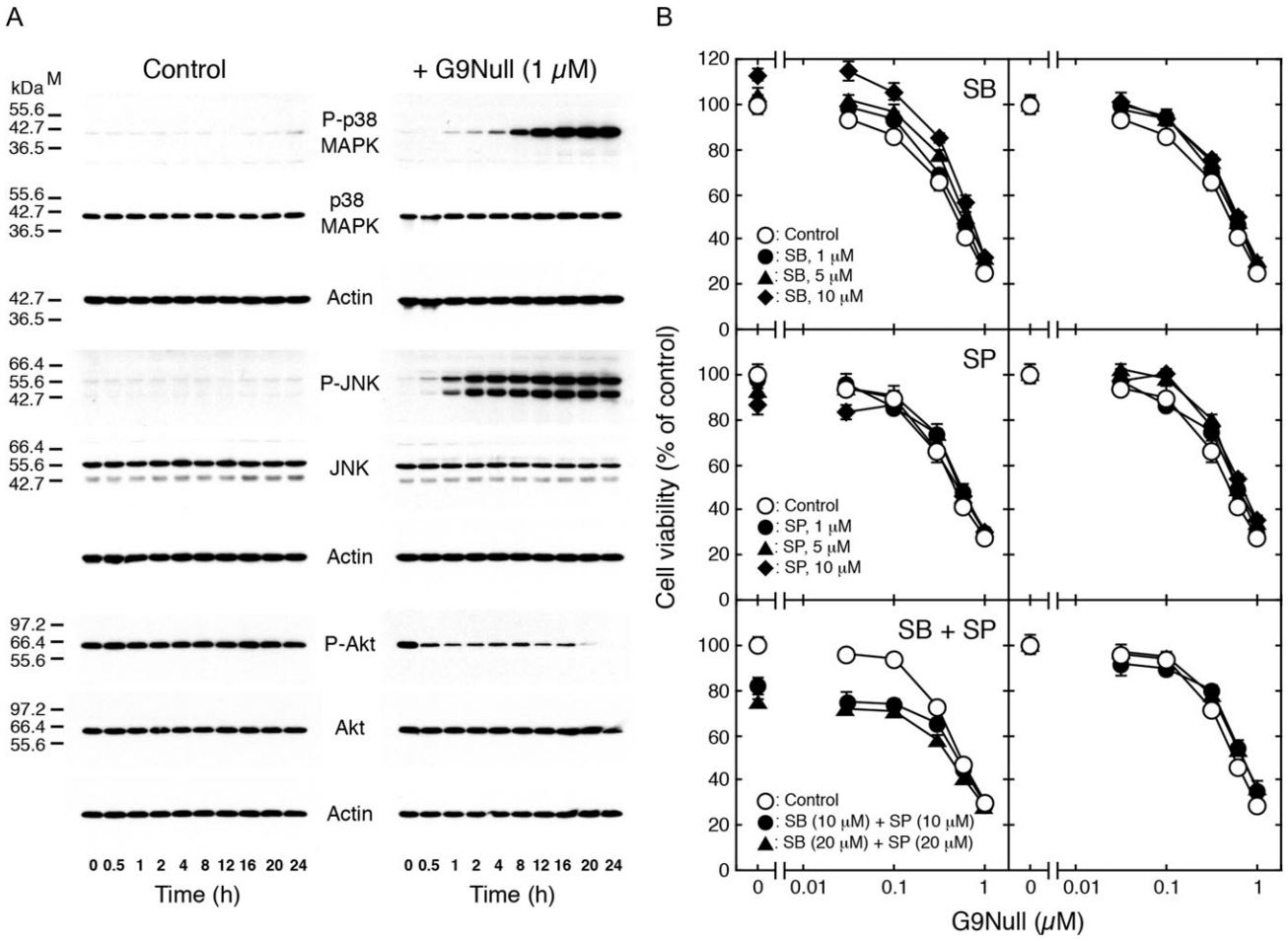

Fig. 2. Gal-9-induced changes in intracellular signaling and the effects of signaling inhibitors on cell death. (**A**) Changes in the phosphorylation status of p38 MAPK, JNK, and Akt in PC-3 cells treated with G9Null (1 μM) were analyzed by western blotting. Whole cell lysates were prepared at the indicated time points after the addition of G9Null. (**B**) A p38 MAPK inhibitor (SB20358) and a JNK inhibitor (SP600125), alone and in combination, were tested as to their ability to suppress Gal-9-induced death in PC-3 cells. The inhibitors were used at the concentrations indicated. G9Null was added after 2-h culture in the presence of the inhibitors. Cell viability was determined by means of the WST-8 assay. The results are presented as mean ± SD (*error bars*). Right panels, the values obtained in the absence of G9Null were taken as 100%. *M*, molecular weight marker proteins; *P-p38 MAPK*, phospho-p38 MAPK (Thr180/Tyr182); *P-JNK*, phospho-JNK (Thr183/Tyr185); *P-Akt*, phospho-Akt (Ser473); *SB*, SB20358; *SP*, SP600125.

Gal-9, respectively. The time courses of phosphorylation of MAPK-activated protein kinase 2 (MAPKAPK-2) and c-Jun, immediate downstream substrates of p38 MAPK and JNK, respectively, were consistent with the results (Supplementary Figure S2). However, SB203580 alone or in combination with a JNK inhibitor (SP600125) exhibited no effect on Gal-9-induced cell death in PC-3 cells (Figure 2B) in spite of near complete suppression of phosphorylation of MAPKAPK-2 and c-Jun by the inhibitors (Supplementary Figure S2).

In addition to those of p38 MAPK and JNK, the phosphorylation status of Akt, another intracellular signaling molecule implicated in apoptosis, was altered by Gal-9. A decrease in the phosphorylated form of Akt was evident within 30 min after the addition of Gal-9 in PC-3 cells and the decreased level continued for at least 24 h (Figure 2A). In the case of Akt, however, a change in phosphorylation of its substrate, Bad (a pro-apoptotic factor), was not detectable (data not shown).

Actin-dependent internalization of Gal-9 and its relation to cell death

Gal-9 added to the culture medium bound to the cell surface in a lactose-sensitive manner (data not shown), and was rapidly internalized and accumulated in PC-3 cells (Figure 3A). After 16-h culture, the internalized Gal-9 colocalized with LAMP-1 indicating that Gal-9 was destined to the lysosomal compartment (Figure 3B). Cytochalasin D, an inhibitor of actin polymerization, disrupted actin filaments with concomitant blockade of Gal-9 internalization (Figure 3A and C). Semi-quantitative western blot analysis (data not shown) revealed that the amount of internalized Gal-9 after 24-h culture had decreased to 27% of the control level in the presence of cytochalasin D. In addition, the cytocidal effect of Gal-9 was mostly completely inhibited in the presence of cytochalasin D in PC-3 cells (Figure 4A). Latrunculin A and jasplakinolide, which affect actin filament dynamics like cytochalasin D, suppressed the growth of PC-3 cells up to 40%, while completely abrogating the effect of Gal-9 (Figure 4A). These actin-targeted agents, however, had negligible effects on the Gal-9-induced apoptotic death of Jurkat cells (Supplementary Figure S3). Unlike the actin-targeted agents, inhibitors of clathrin-mediated endocytosis (CME), dynasore and Pitstop 2, showed ambiguous effects on Gal-9-induced cell death in PC-3 cells: dynasore moderately inhibited it while Pitstop 2 did not affect the cytocidal action of Gal-9 (Figure 4B). Changes in the morphology of actin filaments was evident in PC-3 cells treated with latrunculin but not in ones treated with dynasore (Figure 3A).

Internalized Gal-9 forms detergent-resistant complexes with cellular components and retains lectin activity

In order to identify the binding partner(s) of internalized Gal-9, we tried to solubilize Gal-9-glycoconjugate complexes from the total membrane fraction of Gal-9-treated PC-3 cells according to the procedure schematically shown in Figure 5A (see also *Materials and methods*). The SDS-PAGE patterns of the subcellular fractions obtained with the procedure are shown in Figure 5B. Unexpectedly, internalized Gal-9 was resistant to solubilization with 1% Triton X-100 (Figure 5C, S2) and 1% Triton X-100 plus 1 M NaCl (Figure 5C, S3), but was almost completely solubilized with 1% Triton X-100 plus lactose (Figures 5C, S4·Lac). Gal-9 could be solubilized with lactose even in the absence of the detergent (data not shown). Lectin blot analysis of subcellular fractions of PC-3 cells revealed the presence of two or more major components with apparent molecular weights of about 150,000 and 80,000 capable of interacting with biotinylated Gal-9 in the cell homogenate (Figure 5D, H). Nearly all the Gal-9-interacting substances were recovered in the S2 fraction, i.e., solubilization with 1% Triton X-100. The substances, however, were detectable in the detergent-extracted insoluble fraction when a larger amount of the fraction was analyzed (Figure 5D, P4*), while the detergent-extracted and lactose-treated insoluble fraction was almost completely devoid of the substances (Figure 5D, P4·Lac*).

Effect of Gal-9 on autophagy

Lysosomal localization of internalized Gal-9 suggests possible involvement of the autophagy process in Gal-9-induced death in PC-3 cells like in the colon carcinoma cell lines reported by Wiersma et al. (2015). Analysis of LC3 revealed that LC3-I (non-lipidated form of LC3) was almost undetectable in control PC-3 cells suggesting elevated autophagic flux under unstimulated conditions (Figure 6A). Gal-9 treatment resulted in a moderate and gradual increase in LC3-II (lipidated form of LC3, a marker for autophagic activity), the peak level being reached around 16-h culture (Figure 6A). The amount of LC3-II in Gal-9-treated cells only marginally increased with chloroquine, and rapamycin and bafilomycin A1 exhibited a negligible effect on it, indicating a weak inhibitory effect of Gal-9 on autophagy flux (Figure 6C). Chloroquine, rapamycin and bafilomycin A1 did not modulate the cytocidal action of Gal-9 on PC-3 cells (data not shown). The effect of Gal-9 on the LC3-II content in Jurkat cells was more prominent than that in PC-3 cells. Gal-9 induced a marked increase in LC3-II within 2 h incubation (Figure 6B). The autophagy- and lysosome-targeted agents hardly affected the LC3-II content also in Gal-9-treated Jurkat cells (Figure 6C).

Autophagosomes and lysosomes were visualized with Cyto-ID green detection reagent 2 and LysoTracker Red DND-99, respectively, in control and Gal-9-treated PC-3 cells (Figure 6D). Changes in the number and morphology of the cell organelles were not evident in Gal-9-treated PC-3 cells. In addition, autophagosome-lysosome fusion events, as evidenced by colocalization of the two signals (orange-yellow signal), were hardly affected by Gal-9 (Figure 6D).

Gal-9 induces atypical ubiquitination

Lysosomes play important roles not only in autophagy but also in the degradation of ubiquitinated proteins (Piper and Katzmann 2007). Gal-9 induced accumulation of ubiquitinated proteins, which reached a maximum level after 8–12 h of culture, in PC-3 cells (Figure 7A). While the ubiquitinated proteins detectable with anti-K48-linkage and -K63-linkage specific polyubiquitin antibodies were hardly affected by Gal-9 (Figure 7A). On the other hand, treatment of PC-3 cells with a proteasome inhibitor (MG-132) resulted in an increase in the ubiquitinated proteins detectable with both anti-ubiquitin and anti-K48-linkage specific polyubiquitin antibodies (Figure 7B). In addition, there was a difference in the intracellular distribution of ubiquitinated proteins between Gal-9-treated and MG-132-treated PC-3 cells. In Gal-9-treated cells, colocalization of ubiquitinated proteins and LAMP-1 was detected, while ubiquitinated proteins in MG-132-treated cells were most likely localized in the cytosol and were almost completely absent from LAMP-1-positive compartments (Figure 8A). Consistent with the observations, cell fractionation experiments revealed that nearly all the ubiquitinated proteins were recovered in the insoluble fraction of Gal-9-treated cells, whereas the predominant part of ubiquitinated proteins was recovered in the soluble fractions of MG-132- and epoxomicin-treated cells

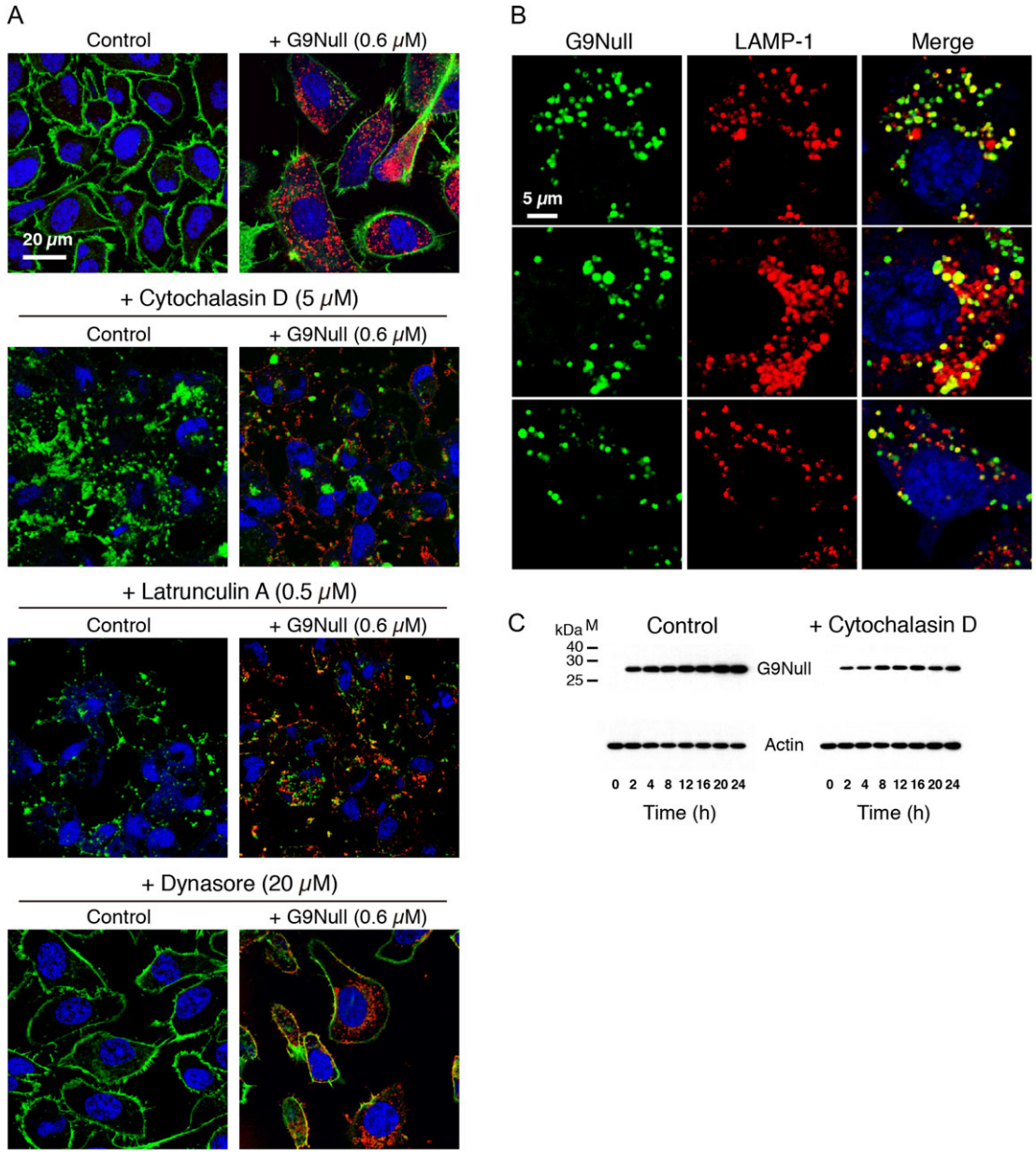

Fig. 3. Immunofluorescence and western blot analyses of internalized Gal-9. (**A**) Confocal microscopic localization of actin and G9Null in PC-3 cells. Cytochalasin D, latrunculin A and dynasore were used at the concentrations indicated. After incubation for 1 h, G9Null was added to a final concentration of 0.6 μM, followed by 16-h culture. Internalized Gal-9 was visualized with anti-Gal-9 rabbit polyclonal antibody and anti-rabbit IgG-Alexa Fluor 568. Actin filaments and nuclei were visualized with fluorescein phalloidin and TO-PRO-3, respectively. (**B**) Confocal microscopic localization of G9Null and LAMP-1 in PC-3 cells. PC-3 cells were treated with G9Null (0.6 μM) for 16 h. LAMP-1 was visualized with anti-LAMP-1 antibody and anti-rabbit IgG-Alexa Fluor 568. Gal-9 was visualized with anti-Gal-9 mouse monoclonal antibody and fluorescein-labeled antibody to mouse IgG. Nuclei were visualized with TO-PRO-3. (**C**) Western blot analysis of internalized G9Null in PC-3 cells. Time-dependent changes in the content of internalized G9Null were determined in the absence and presence of cytochalasin D (5 μM). Cell lysates were prepared at indicated time points after the addition of G9Null (0.6 μM). Cells were washed twice with PBS, 0.2 M lactose to remove extracellular G9Null before preparation of cell lysates. *M*, molecular weight marker proteins.

(Figure 8B). Analysis of the subcellular fractions shown in Figure 5A demonstrated that although most of the ubiquitinated proteins in Gal-9-treated cells were solubilized with the detergent, i.e., recovered in the S2 fraction, they were detectable in the P4/P4* fraction (Figure 8C), and that the content of the ubiquitinated proteins in P4·Lac/P4·Lac* was apparently lower than that in the P4/P4* fraction. These results prompted us to examine the effect of a ubiquitination inhibitor on Gal-9-induced cell death in PC-3 cells. Time-course experiments showed that PYR-41, a ubiquitin-activating enzyme (E1) inhibitor, suppressed accumulation of ubiquitinated proteins up to 8 h in Gal-9-treated PC-3 cells (Figure 9A). After that, the contents of ubiquitinated proteins increased to or above those in cells treated with Gal-9 alone. In spite of the incomplete inhibition of ubiquitination, PYR-41 abrogated the cytocidal effect of Gal-9 in the cells (Figure 9B). The inhibitors of actin filament dynamics, which suppressed Gal-9-induced cell death in PC-3 cells, were evaluated for their ability to inhibit ubiquitination in order to elucidate the relationship between ubiquitination and cell death. The suppressive capability of jasplakinolide as to Gal-9-induced ubiquitination was

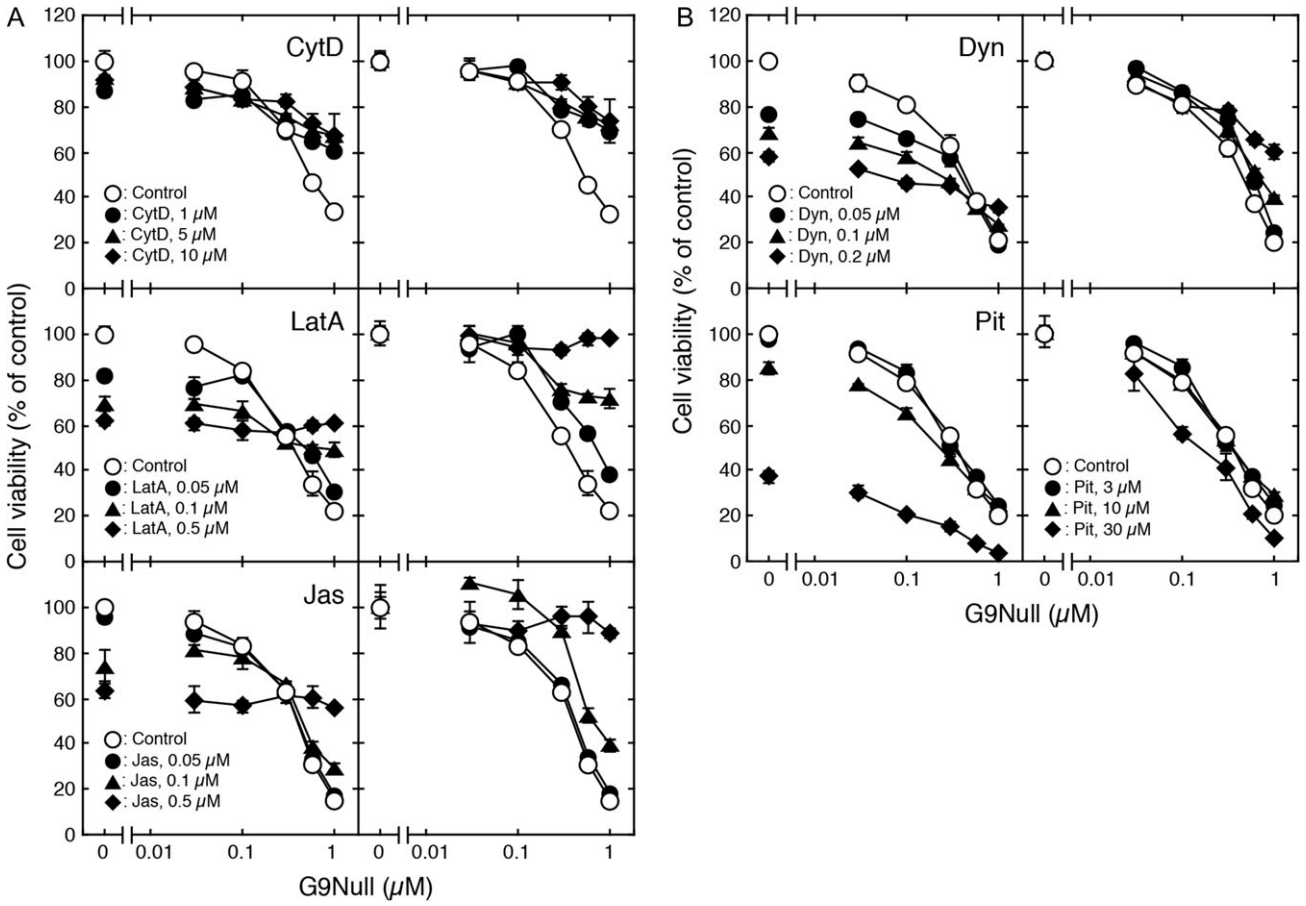

Fig. 4. Effects of endocytosis inhibitors on Gal-9-induced death in PC-3 cells. (**A**, **B**) Endocytosis inhibitors were added at the concentrations indicated. G9Null was added after 1-h culture. Cell viability was determined by means of the WST-8 assay. The results are presented as mean ± SD (*error bars*). Right panels, the values obtained in the absence of G9Null were taken as 100%. *CytD*, cytochalasin D; *LatA*, latrunculin A; *Jas*, jasplakinolide; *Dyn*, dynasore; *Pit*, Pitstop 2.

comparable to or higher than that of PYR-41 after 8-h culture (Figure 9C). In contrast, cytochalasin D and latrunculin A exhibited no or only a limited influence on the ubiquitination under the conditions used. Accumulation of ubiquitinated proteins was also detectable in Jurkat cells treated with Gal-9, although quantitative comparison of the ubiquitination levels between PC-3 and Jurkat cells was not performed (Supplementary Figure S4). PYR-41, however, did not prevent Gal-9-induced apoptotic death in Jurkat cells.

Discussion

The molecular mechanisms underlying Gal-9-induced cell death have been studied mainly in lymphoid cell lines based on its unique role as an immune modulator. Although there are still several controversial issues that need to be clarified, it is generally accepted that Gal-9 triggers the apoptotic process in the cells (Wiersma et al. 2013). Studies regarding non-lymphoid cell lines, however, suggest the existence of multiple mechanisms (apoptotic and non-apoptotic) in Gal-9-induced cell death depending on the cell type (Wiersma et al. 2015; Fujita et al. 2017). The present results indicate that Gal-9 induced non-apoptotic death in PC-3 cells. Several low molecular weight apoptosis inducers tested in this study also failed to induce the apoptotic process leading to DNA fragmentation. However, piplartine (a plant alkaloid) (Kong et al. 2008), maysin (a flavonoid) (Lee et al. 2014), and other compounds have been shown to induce apoptotic responses including caspase-3 activation and DNA fragmentation in PC-3 cells, indicating that the cell line is not totally resistant to apoptosis but has the molecular machinery necessary to undergo the process upon proper stimulation.

Gal-9 initiated an intracellular signaling pathway(s) leading to activation of p38 MAPK and JNK in PC-3 cells. Kobayashi et al. reported the participation of p38 MAPK and JNK signaling in Gal-9-induced cell death in myeloma cell lines (Kobayashi et al. 2010). Many types of cellular stressors of external and internal origin are known to activate the p38 MAPK and JNK pathways, and their activation has been implicated in apoptosis of mammalian and lower eukaryotic cells (Takeda et al. 2008). Although phosphorylation of p38 MAPK and JNK was markedly upregulated by Gal-9 in PC-3 cells, the results obtained using their inhibitors, SB203580 and SP600125, suggest that activation of the signaling pathways is dispensable for Gal-9-induced death in PC-3 cells. The inability of the inhibitors to suppress the effect of Gal-9 was not due to insufficient inhibition of the kinases, because the compounds markedly inhibited phosphorylation of MAPKAPK-2 and c-Jun, immediate downstream substrates of p38 MAPK and JNK, respectively (Supplementary Figure S2).

The phosphatidylinositol 3-kinase (PI3K)-Akt pathway is essential for cell growth and survival, and implicated in apoptosis (Franke et al. 2003). Akt plays an anti-apoptotic role under a variety of conditions, including withdrawal of extracellular growth-

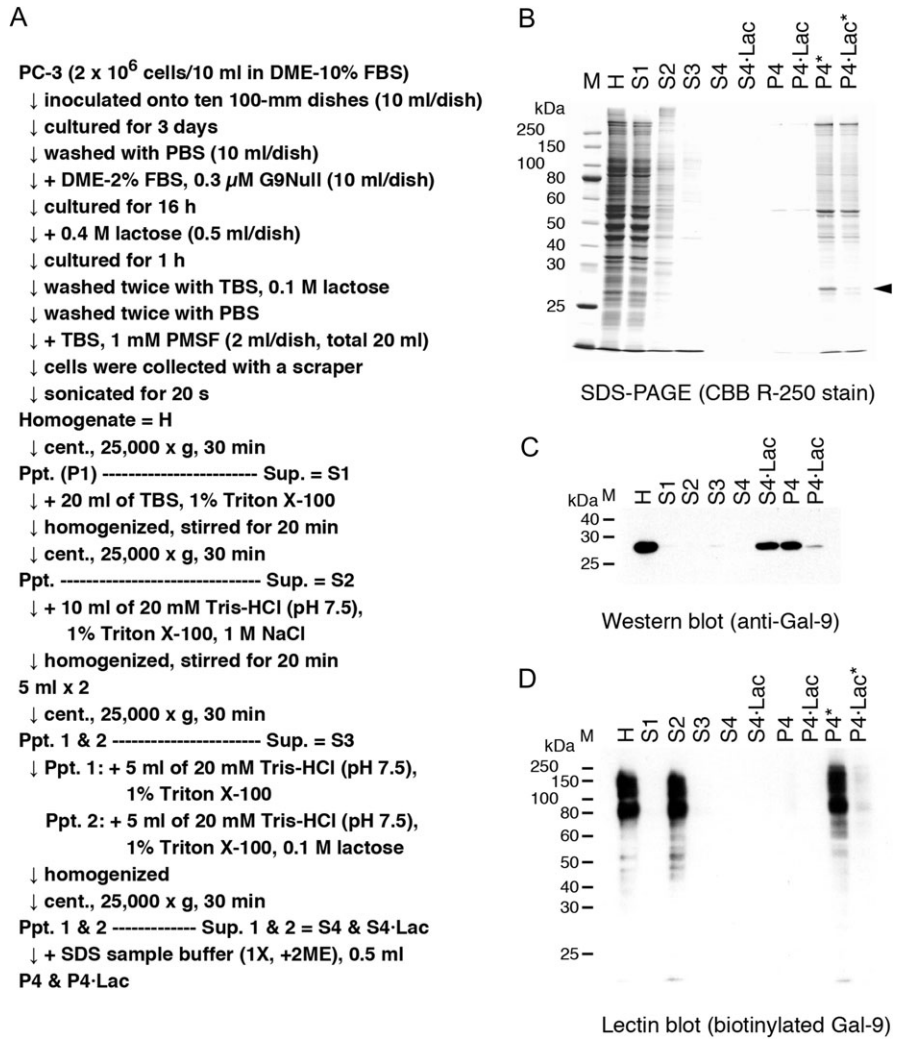

Fig. 5. Subcellular fractionation of PC-3 cells treated with Gal-9. (**A**) Schematic representation of the subcellular fractionation procedure for PC-3 cells treated with Gal-9. (**B**) Samples were analyzed by SDS-PAGE (10% gel) and then stained with Coomassie brilliant blue R-250. An arrowhead shows the position of G9Null. (**C**) Western blot analysis of Gal-9. *D,* lectin blot analysis using biotinylated Gal-9 as a probe. *M,* molecular weight marker proteins; *H ~ P4·Lac,* cellular components derived from ca. 3×10^4 cells/lane; *P4** and *P4·Lac*,* cellular components derived from ca. 2.4×10^5 cells/lane.

stimulating signals, and increased stress of both extracellular and intracellular origin. Akt can maintain mitochondrial integrity by inactivating pro-apoptotic factors such as Bad, which leads to prevention of apoptosis. Treatment with Gal-9 resulted in a rapid and sustained decrease in phosphorylated Akt but the phosphorylation of Bad (at Ser112 and/or Ser136) was not affected in PC-3 cells (data not shown). Nevertheless, we cannot exclude the possible involvement of the PI3K-Akt pathway in Gal-9 induced cell death because Akt regulates not only Bad but also a wide variety of downstream effector molecules.

Receptor-mediated endocytosis can be roughly divided into two types, namely CME and clathrin-independent endocytosis (CIE) (Dutta and Donaldson 2012; Johannes et al. 2015). CME, as the name implies, is a process requiring the formation of clathrin-coated vesicles. While CIE includes several distinct endocytic pathways that depend on actin filament dynamics. The lactose-sensitive nature of Gal-9 internalization indicates that the interaction between Gal-9 and cell surface glycoconjugate(s) (most likely glycoproteins) is indispensable for the process. Agents capable of inhibiting actin dynamics, i.e., dynamic polymerization and depolymerization of actin filaments (cytochalasin D, latrunculin A, and jasplakinolide), inhibited both Gal-9 internalization and Gal-9-induced death in PC-3 cells (Figures 3A and 4A). The results suggest that Gal-9 internalized via CIE is closely associated with the cytocidal action, although the precise mechanism of internalization remains unclear. The inhibitory effect of dynasore on Gal-9-induced cell death is not inconsistent with the results: dynasore inhibits the GTPase activity of dynamin, which is required for not only the scission of clathrin-coated vesicles in CME but also the caveolar endocytosis in CIE (Bastiani and Parton 2010).

Tim-3 (T-cell immunoglobulin mucin-3), CD44 and GLUT2 (glucose transporter 2) are cell membrane glycoproteins supposed to act as receptors/binding partners for Gal-9 (Ohtsubo et al. 2005; Zhu et al. 2005; Katoh et al. 2007). In most cell types, however, the receptor(s) for Gal-9 responsible for transducing cytocidal signals has not been identified. We tried to isolate the Gal-9-receptor complex from PC-3 cells on the assumption that the complex stably exists in intracellular vesicles including lysosomes. Contrary to our expectation, internalized Gal-9 was

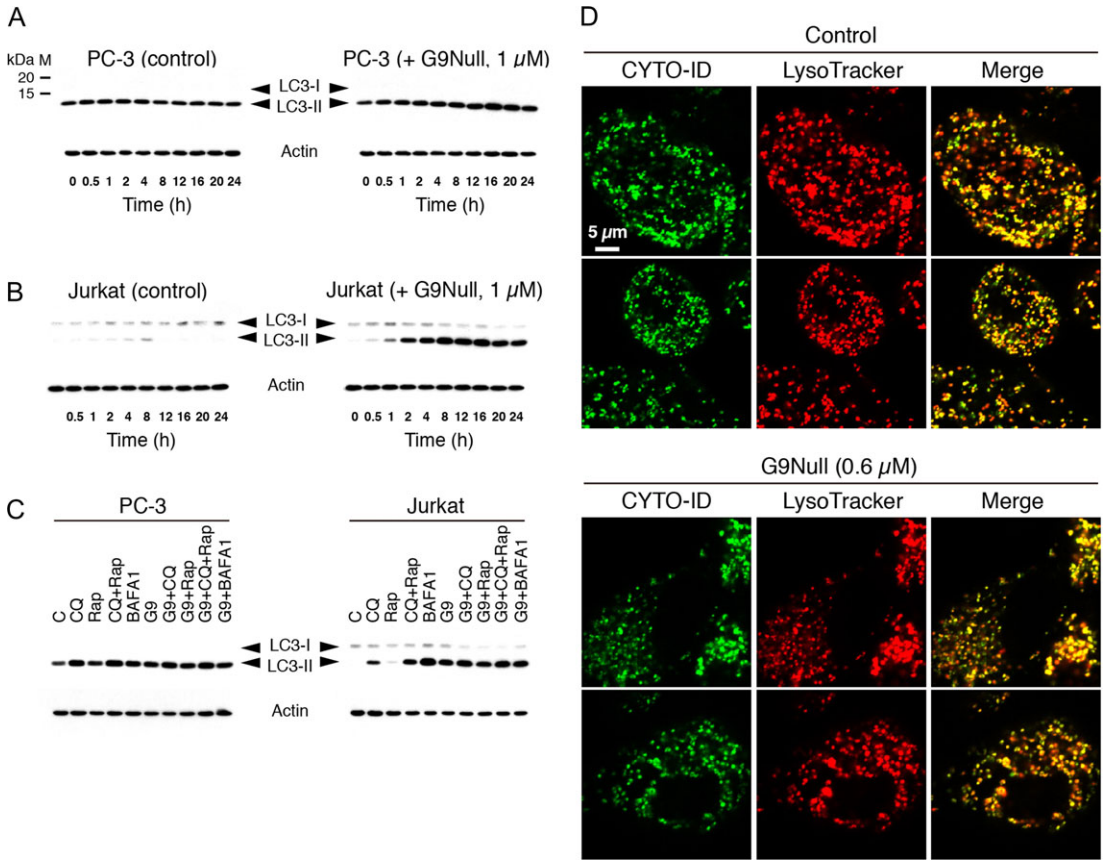

Fig. 6. Effect of Gal-9 on the autophagic process in PC-3 and Jurkat cells. (**A** and **B**) Time-dependent changes in the contents of LC3-I and -II were analyzed by western blotting. PC-3 (*A*) and Jurkat (*B*) cells were treated with G9Null (1 μM) for up to 24 h. Whole cell lysates were prepared at the time points indicated. (**C**) Whole cell lysates were prepared from PC-3 and Jurkat cells cultured in the presence of the indicated reagents for 16 h. (**D**) Confocal microscopic localization of autophagosomes and lysosomes in PC-3 cells. PC-3 cells were cultured in the absence and presence of G9Null (0.6 μM) for 16 h. Autophagosomes and lysosomes were visualized with CYTO-ID Green Detection Reagent 2 and LysoTracker Red DND-99, respectively. *M*, molecular weight marker proteins; *C*, control; *CQ*, 10 μM chloroquine; *Rap*, 0.5 μM rapamycin; *BAFA1*, 0.2 μM bafilomycin A1; *G9*, 1 μM G9Null.

resistant to solubilization with a detergent (Figure 5). This was not due to the formation of insoluble aggregates of denatured Gal-9, because internalized Gal-9 was almost completely solubilized from the membrane fraction with lactose regardless of the presence of a detergent. The results indicate that internalized Gal-9 is not denatured but retains lectin activity. In addition, candidate Gal-9 receptors with apparent molecular weights of about 150,000 and 80,000 found on lectin blot analysis were clearly detected in P4 (insoluble fraction after extraction with Triton X-100) but nearly absent in P4·Lac (insoluble fraction after extraction with Triton X-100 plus lactose) (Figure 5D). These results suggest that the candidate receptors crosslinked by Gal-9 exist as detergent-resistant stable complexes likely in endosomes and lysosomes.

Wiersma et al. reported that Gal-9 exhibited a cytocidal effect on KRAS (Kirsten rat sarcoma 2 viral oncogene homolog) mutant colorectal cancer (CRC) cells by inhibiting the last steps of the autophagic process (Wiersma et al. 2015). Gal-9 added to the culture medium was rapidly internalized and accumulated in the lysosomal compartment in CRC cells. Gal-9 inhibited autophagosome-lysosome fusion, which resulted in autophagosome accumulation, lysosomal swelling and cell death in KRAS mutant CRC cells. Their observations, i.e., the non-apoptotic nature of Gal-9-induced cell death and endocytic internalization leading to lysosomal accumulation of Gal-9, are consistent with the results obtained in the present study. On the other hand, Gal-9 exhibited a negligible effect on autophagosome-lysosome fusion events in PC-3 cells (Figure 6D). In addition, a marked increase in the lipidated form of LC3 (LC3-II) in CRC cells upon treatment with Gal-9 was not observed in PC-3 cells: nearly all LC3 existed as LC3-II in unstimulated PC-3 cells, and treatment with Gal-9 resulted in only a moderate to small increase in the LC3-II content (Figure 6A). It seems most likely that Gal-9-induced changes in autophagic flux, if any, are not a major cause of death in PC-3 cells.

The autophagy-lysosome and ubiquitin-proteasome systems are two major intracellular protein degradation systems in eukaryotic cells. Protein ubiquitination is an enzymatic cascade reaction in which the C-terminus of ubiquitin, a small protein of 76-amino acids, is covalently attached to the lysine residue(s) of a substrate via an isopeptide bond, resulting in the formation of a monoubiquitinated/multi-monoubiquitinated protein. Further modification of the N-terminus (methionine residue) or one of the seven lysine residues (K6, K11, K27, K29, K33, K48 and K63) of the substrate-attached ubiquitin moiety leads to the formation of polyubiquitin chains with different structures (Komander and Rape 2012). The polyubiquitin chains might be branched or linear and either homogeneous or heterogeneous (mixed) with respect to linkages. Ubiquitination has multiple functions including in protein degradation, signal transduction, and regulation of the cell cycle, which depends on the modification type, i.e., mono- or poly-ubiquitination, homogeneous or mixed

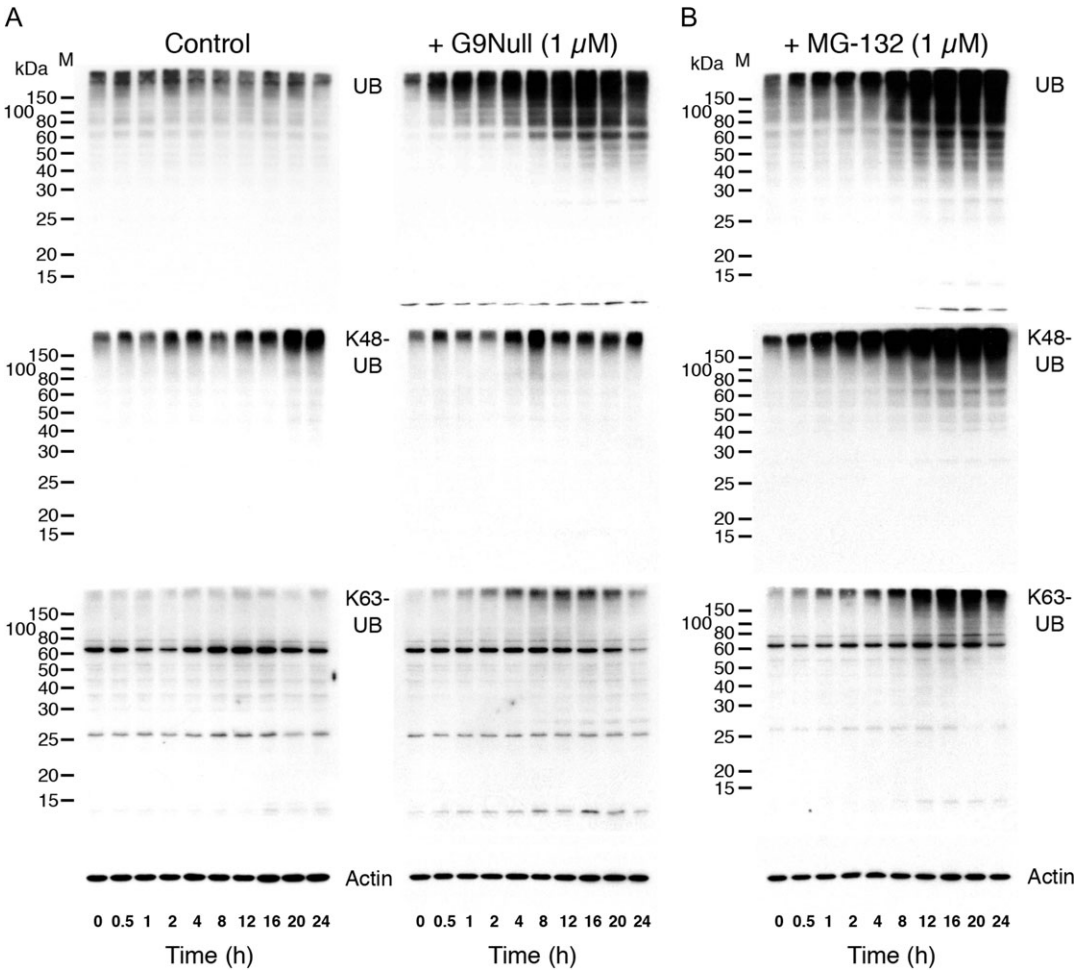

Fig. 7. Effects of Gal-9 and a proteasome inhibitor on ubiquitination in PC-3 cells. (**A** and **B**) PC-3 cells were treated with G9Null (1 μM) (A, right panels) and MG-132 (1 μM) (B) for up to 24 h. Whole cell lysates prepared at the time points indicated were subjected to western blot analysis. *M,* molecular weight marker proteins; *UB,* ubiqutin; *K48-UB,* K48-linked polyubiquitin; *K63-UB,* K63-linked polyubiquitin.

linkage, etc. From a simplified point of view, the K48-linked polyubiquitin chain directs the substrate for proteasomal degradation, while linear (M1-) and K63-linked polyubiquitin chains facilitate protein complex formation and modulate intracellular signal transduction. The functions of K6-/K27-/K29-/K33-linked ubiquitin and branched ubiquitin chains are less understood. Although a typical role of ubiquitination is to mediate degradation by proteasomes, some ubiquitinated proteins, such as activated membrane receptors, are endocytosed and directed to lysosomal degradation (Dikic and Giordano 2003). We analyzed ubiquitinated proteins in whole cell lysates, and soluble and insoluble fractions of PC-3 cells to examine the possibility that Gal-9 modulates the ubiquitination system. Gal-9 caused time-dependent accumulation of ubiquitinated proteins in a similar manner to MG-132, a proteasome inhibitor (Figure 7). However, there were differences between ubiquitinated proteins accumulated upon treatment with Gal-9 and those with MG-132: (i) Ubiquitinated proteins in Gal-9-treated and MG-132-treated cells were recovered mainly in the insoluble and soluble fractions, respectively. Likewise, ubiquitinated proteins accumulated upon treatment with epoxomicin, another proteasome inhibitor, were recovered mainly in the soluble fraction. (ii) Colocalization of ubiquitinated proteins and LAMP-1 was detectable in Gal-9-treated but not MG-132-treated cells. (iii) MG-132 induced accumulation of ubiquitinated proteins carrying K48-linked polyubiquitin (an essential signal for proteasomal degradation), while Gal-9 hardly affected the contents of those carrying K48-linked and K63-linked polyubiquitin. Although we have not tested other linkage-specific polyubiquitin antibodies (K11-, K27-, M1-/linear, etc.), it is probable that Gal-9 stimulated heterogeneous/mixed-type ubiquitination and/or monoubiquitination/multi-monoubiquitination (Dikic and Giordano 2003; Ohtake and Tsuchiya 2017). In addition, PYR-41, which inhibits the first step of ubiquitination, suppressed Gal-9-induced accumulation of ubiquitinated proteins up to 8 h and abrogated the cytocidal effect of Gal-9 in PC-3 cells. The presence of larger amounts of ubiquitinated proteins in P4 than in P4·Lac implies that they form insoluble complexes with Gal-9 in lysosomes (Figure 8C). The results shown in Figure 8C indicate that the recovery of ubiquitinated proteins into subcellular fractions (S1–S4 and P4) is significantly low, although quantitative analysis was not performed. Currently, we cannot fully explain the discrepancy. One possible explanation is that the ubiqutin moieties of ubiquitinated proteins were released by deubiquitinating enzymes (DUBs) during cell fractionation. In addition, it is also possible that the released ubiquitin moieties were degraded by proteases in S1 and S2 fractions.

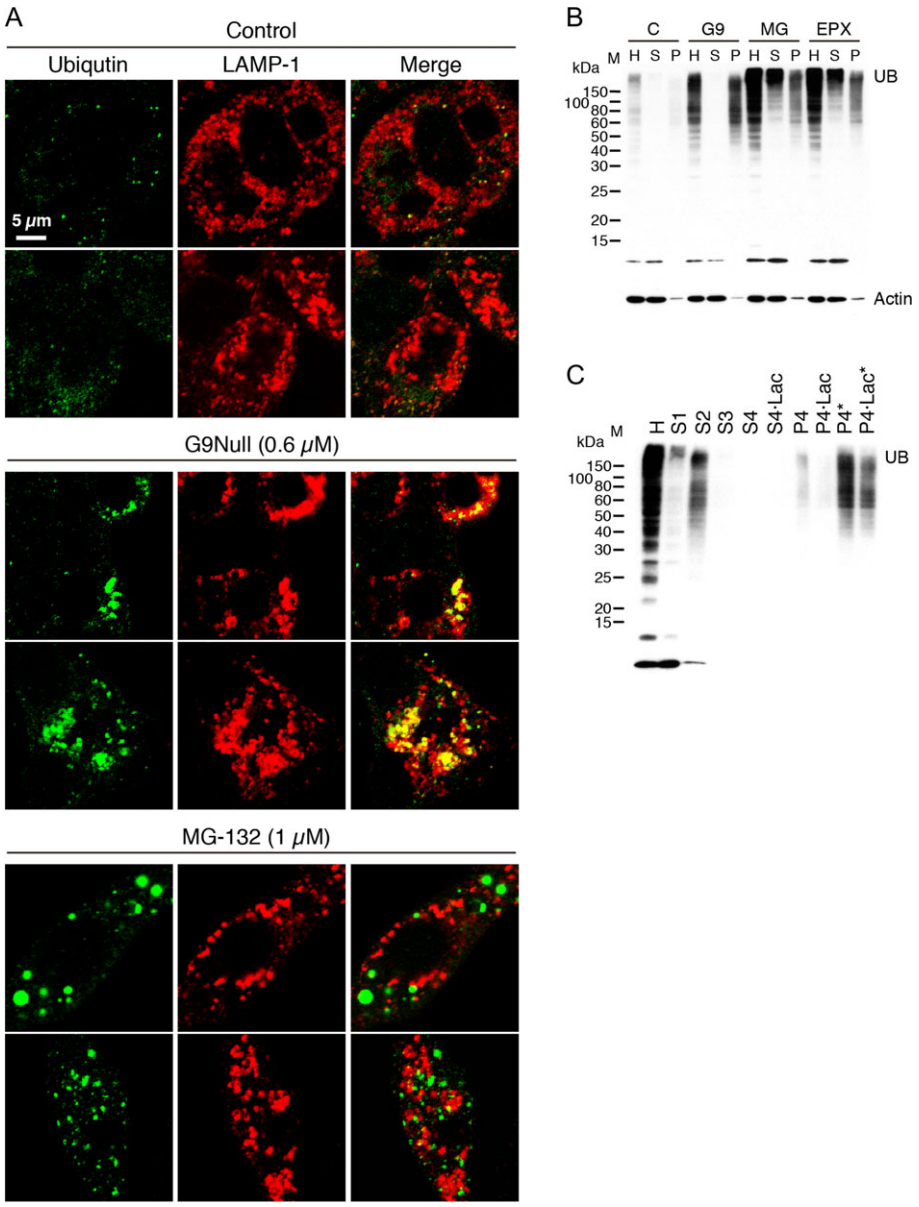

Fig. 8. Subcellular localization of ubiquitinated proteins in PC-3 cells. (**A**) Confocal microscopic localization of ubiquitinated proteins and LAMP-1. PC-3 cells were treated with G9Null (0.6 μM) and MG-132 (1 μM) for 16 h. Ubiquitin was visualized with anti-ubiquitin mouse monoclonal antibody and fluorescein-labeled antibody to mouse IgG. LAMP-1 was visualized with anti-LAMP-1 antibody and anti-rabbit IgG-Alexa Fluor 568. (**B**) Subcellular localization of ubiquitinated proteins was analyzed by western blotting. Homogenate (H), soluble fractions (S) and total membrane fractions (P, P1 fraction in Figure 5A) were prepared from PC-3 cells treated with the indicated reagents for 16 h according to the procedure shown in Figure 5A. (**C**) The subcellular fractions shown in Figure 5A were subjected to western blot analysis using anti-ubiquitin monoclonal antibody. *M*, molecular weight marker proteins; *C*, control; *G9*, 1 μM G9Null; *MG*, 1 μM MG-132; *EPX*, 50 nM epoxomicin; *UB*, ubiquitin; *H ~ P4·Lac*, cellular components derived from ca. 3×10^4 cells/lane; *P4** and *P4·Lac**, cellular components derived from ca. 2.4×10^5 cells/lane.

These results suggest that Gal-9-induced atypical ubiquitination and the accumulation of the ubiquitinated proteins in the lysosomal compartment play a pivotal role in Gal-9-induced death in PC-3 cells. The inconsistent results regarding the influence of actin inhibitors (cytochalasin D and latrunculin A, Figure 9C) on Gal-9-induced ubiquitination indicate that upregulation of atypical ubiquitination is not a sufficient condition to efficiently induce cell death and that endocytosed Gal-9 plays an indispensable role in the cytocidal action. Currently, the molecular mechanisms by which Gal-9 stimulates ubiquitination and modification type(s) of Gal-9-induced ubiquitination are unclear. Nevertheless, we hypothesize that Gal-9-induced crosslinking of cell surface receptors/binding partners causes mixed type ubiquitination and/or monoubiquitination/multi-monoubiquitination of membrane proteins. A part of the ubiquitinated proteins in association with Gal-9 internalize and accumulate as detergent-resistant complexes in the lysosomal compartment, which result in malfunction of lysosomes and lysosome-dependent processes in PC-3 cells.

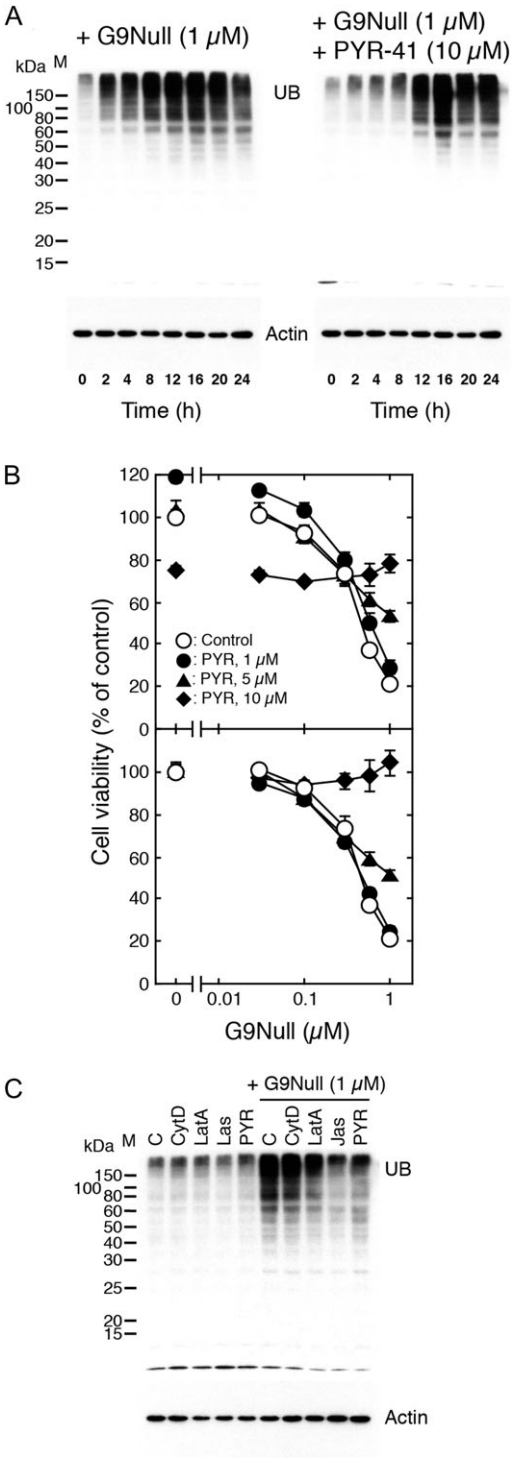

Fig. 9. Effects of a ubiquitination inhibitor and actin inhibitors on Gal-9-induced ubiquitination and cell death in PC-3 cells. (**A**) PC-3 cells were treated with G9Null (1 μM) and G9Null (1 μM) plus PYR-41 (10 μM) for up to 24 h. Whole cell lysates prepared at the time points indicated were subjected to western blot analysis. (**B**) PYR-41 was tested as to its ability to suppress Gal-9-induced death in PC-3 cells. PYR-41 was added at the concentrations indicated. G9Null was added after 2-h culture. Cell viability was determined by means of the WST-8 assay. The results are presented as mean ± SD (*error bars*). Lower panel, the values obtained in the absence of G9Null were taken as 100%. (**C**) PC-3 cells were treated with G9Null (1 μM) in the presence and absence of actin inhibitors for 8 h. Whole cell lysates were subjected to western blot analysis. *M*, molecular weight marker proteins; *UB*, ubiquitin; *C*, control; *CytD*, 5 μM cytochalasin D; *LatA*, 0.5 μM latrunculin A; *Jas*, 0.5 μM jasplakinolide; *PYR*, 10 μM PYR-41.

Materials and methods

Reagents and antibodies

Primary antibodies against the following proteins were purchased from Cell Signaling Technology (Danvers, MA, USA): β-actin (#4967), JNK (#9252), phospho-JNK (Thr183/Tyr185) (#4668), c-Jun (#9165), phospho-c-Jun (Ser63) (#2361), p38 MAPK (#9212), phospho-p38 MAPK (Thr180/Tyr182) (#9211), MAPKAPK-2 (#12155), phospho-MAPKAPK-2 (Thr334) (#3007), Akt (#9272), phospho-Akt (Ser473) (#9271), LC3A/B (#12741), LAMP-1 (#9091), ubiquitin (#3936; mouse monoclonal antibody), K48-linked polyubiquitin (#8081), K63-linked polyubiquitin (#5621), caspase 3 (#9665), cleaved caspase 3 (Asp175) (#9664), Bad (#9239), and phospho-Bad (Ser112 and Ser136) (#5284 and #4366). The mouse monoclonal antibody raised against the N-terminal CRD of Gal-9 was donated by Fuso Pharmaceutical Industries, Ltd. (Osaka, Japan). Cytochalasin D and latrunculin A were from Wako Pure Chemical Industries (Osaka, Japan). Jasplakinolide, SP600125, SB203580, and MG-132 were from Cayman Chemical (Ann Arbor, MI, USA). Dynasore, Pitstop 2 and PYR-41 were from Abcam. Epoxomicin was obtained from Merck (Darmstadt, Germany).

Expression and purification of recombinant proteins

Expression of tag-free recombinant proteins, CSGal-1, G9Null, and other members of the human galectin family except for Gal-4, in *Escherichia coli* BL21(DE3) was carried out as described previously (Nishi et al. 2005, 2008). Recombinant proteins were purified by affinity chromatography on a lactose-agarose column (Seikagaku Corp., Tokyo, Japan). Gal-4 was expressed as a glutathione S-transferase (GST)-fusion protein and purified by affinity chromatography on a glutathione-Sepharose column (GE Healthcare, Piscataway, NJ, USA). The GST tag was removed by thrombin cleavage. The purified proteins were dialyzed against PBS and then sterilized by filtration. The protein concentrations were determined using BCA protein assay reagent (Pierce, Rockford, IL, USA) and BSA as a standard.

Cell culture and cell viability assays

The human prostatic cancer cell line (PC-3) was provided by the RIKEN BioResource Center (Ibaraki Japan). The Jurkat T lymphoma cell line was obtained from the American Type Culture Collection (Manassas, VA, USA). PC-3 cells were maintained in Dulbecco's modified Eagle's medium (DMEM) supplemented with 10% FBS, 100 mU/mL penicillin and 100 μg/mL streptomycin (DMEM-10% FBS) at 37°C under a 5% CO_2 – 95% atmosphere. Jurkat cells were maintained in RPMI 1640 supplemented with 10% FBS, 100 mU/mL penicillin and 100 μg/mL streptomycin (RPMI 1640-10% FBS).

The cytocidal effects of Gal-9 and other substances on PC-3 cells were determined by means of the WST-8 assay. Trypsinized PC-3 cells were centrifuged and then resuspended in DMEM-2% FBS at a cell density of 1×10^4 cells/90 μL. The cell suspension was plated onto 96-well plates (90 μL/well) and then cultured for 24 h. Test samples (10 μL) were added at various concentrations, and the cultures were continued for 24 h unless otherwise stated. WST-8

reagent (Cell counting kit-8; Dojin Laboratories, Kumamoto, Japan) was added to the cells (10 μL), followed by incubation for 2 h. Each assay was performed in triplicate. The viable cell number was determined as the difference between the absorbance at 450 nm and 620 nm using a microplate reader. Jurkat cells were centrifuged and then resuspended in RPMI 1640-10% FBS at a cell density of 3×10^4 cells/90 μL. The cell suspension was plated onto 96-well plates (90 μL/well) and then cultured for 2 h. Test samples (10 μL) were added at various concentrations, and the cultures were continued for 24 h unless otherwise stated. The WST-8 assay was carried out as described above in this section.

SDS-PAGE, western blot and lectin blot analyses

Samples and standards (10 μL/lane) were electrophoretically separated in SDS/12.6% polyacrylamide gels under reducing conditions unless otherwise specified. The gels were stained with Coomassie Brilliant Blue R-250. Two protein ladder markers (P7701 and P7703; New England Biolabs, Inc., Beverly, MA, USA) were used in this study. Note that the molecular weight of G9Null estimated by using the molecular weight marker proteins is significantly lower than the actual value (33,100) (Figures 3C, 5B, and 5C). For western blot analysis, samples were electrophoretically separated as described above in this section and then transferred to polyvinylidene difluoride (PVDF) membranes (Millipore Corp., Billerica, MA, USA), followed by immunodetection with primary antibodies and horseradish peroxidase-labeled goat anti-rabbit/mouse IgG antibody (Kirkegaard and Perry Laboratories, Gaithersburg, MD, USA). The membranes were blocked with TBS (Tris-buffered saline; 20 mM Tris-HCl, 0.15 M NaCl, pH 7.5), 5% skim milk for 1 h before incubation with primary antibodies. Immunoreactive bands were visualized using an ECL detection system (GE Healthcare). When necessary, blots were stripped at 50°C for 30 min in 50 mM Tris-HCl (pH 6.8), 2% SDS, 0.1 M β-mercaptoethanol, followed by washing with TBS. The stripped membranes were blocked with TBS, 5% skim milk for 30 min before reprobing. A homemade affinity-purified rabbit polyclonal antibody raised against the C-terminal CRD of Gal-9 was used for the detection of Gal-9 on western blot analysis. For semi-quantitative western blot analysis of internalized G9Null, serially diluted samples were electrophoresed with the standard G9Null (0.5, 1, 2, and 5 ng/lane). The visualized bands were scanned and quantitated using ImageJ software (Abramoff et al. 2004). Lectin blot analysis was carried out as described by Matsumura et al. (2007) with modifications. G9Null was biotinylated using EZ-Link NHS-Biotin (Pierce) according to the manufacturer's instructions. Samples were electrophoretically separated as described above in this section and then transferred to PVDF membranes. The membranes were blocked with TBS, 1% BSA for 1 h, and then incubated overnight with 1 μg/mL of biotinylated G9Null in TBS-T (TBS containing 0.05% Tween 20). After washing with TBS-T, the membranes were incubated with streptavidin-biotinylated horseradish peroxidase complex (GE Healthcare) for 1 h, and then washed with TBS-T. Chemiluminescent detection was carried out using an ECL detection system.

Whole cell lysates subjected to SDS electrophoretic analyses were prepared as follows: PC-3 cells suspended in DMEM-2% FBS (1×10^5 cells/0.9 mL) were plated onto 12-well plates (0.9 mL/well) and then cultured for 24 h. After adding test samples (100 μL), cells were cultured for various lengths of time (up to 24 h). After removing the medium, the cells were lysed with 100 μL of 1X SDS sample buffer. Jurkat cells suspended in RPMI 1640-10% FBS (3×10^5 cells/0.9 mL) were plated onto 12-well plates (0.9 mL/well) and then cultured for 2 h. After adding test samples (100 μL), cells were cultured for various lengths of time (up to 24 h). At the end of the culture period, cells were transferred to 1.5-mL tubes and then centrifuged at $2000 \times g$ for 30 s using a table-top mini centrifuge. After removing the supernatant, each cell pellet was lysed with 100 μL of 1X SDS sample buffer.

Agarose gel electrophoresis for DNA fragmentation assay

PC-3 cells suspended in DMEM-2% FBS at a cell density of 7.5×10^5 cells/1.8 mL were plated onto a 6-well plate (1.8 mL/well) and then cultured for 24 h. After adding test samples (PBS, 20 μM actinomycin D, and 10 μM G9Null: 200 μL/well), the cultures were continued for 24 h. Cells were trypsinized and then lysed in 50 mM Tris-HCl (pH 8.0), 10 mM EDTA, 0.5% (w/v) *N*-lauroyl sarcosine sodium salt, followed by treatment with RNase A (0.5 mg/mL) at 50°C for 30 min and then with Proteinase K (0.4 mg/mL) at 50°C for 1 h. The resulting cell digests were analyzed by 2% agarose gel electrophoresis. DNA fragments were stained with ethidium bromide. Jurkat cells suspended in RPMI 1640-10% FBS at a cell density of 1.5×10^6 cells/0.9 mL were plated onto a 12-well plate (0.9 mL/well) and then cultured for 2 h. After adding test samples (100 μL/well), the cultures were continued for 24 h. Jurkat cells collected by centrifugation were lysed and treated with RNase A and Proteinase K as described above in this section before analysis by agarose gel electrophoresis.

Subcellular fractionation of PC-3 cells treated with Gal-9

PC-3 cells suspended in DMEM-10% FBS (2×10^6 cells/10 mL) were inoculated into ten 100-mm dishes (10 mL/dish) and then cultured for 72 h. After removing the medium, the cells were cultured for 16 h with DMEM-2% FBS containing 0.3 μM G9Null (10 mL/dish). The concentration, 0.3 μM, was used to minimize the influence of G9Null non-specifically bound to the cell surface, which could not be removed with lactose. At the end of the culture period, the 0.4 M lactose solution (0.5 mL/dish) was added to the medium, followed by 1-h culture. The cell number at the end of the culture period was determined to be $7.8 \pm 0.7 \times 10^6$ cells/dish (3.1 ± 0.3 mg protein/dish) using replicate dishes ($n = 3$). After removing the medium, the cells were washed twice with TBS, 0.1 M lactose and then twice with PBS (10 mL/dish). The following procedure was carried out under ice-cold conditions. The washed cells were collected with a scraper using a homogenizing buffer (TBS, 1 mM phenylmethylsulfonyl fluoride, 2 mL/dish). The cell suspension (total 20 mL) was sonicated for 30 s with a model XL-7000 sonicator (Qsonica, Newtown, CT, USA) (output intensity = 1) and then centrifuged. All centrifugation was performed at $25{,}000 \times g$ for 30 min. Each resulting pellet was homogenized with 20 mL of TBS, 1% Triton X-100 using a Teflon-glass homogenizer. The homogenate was stirred for 20 min, followed by centrifugation. The resulting pellet was homogenized with 10 mL of 20 mM Tris-HCl (pH 7.5), 1% Triton X-100, 1 M NaCl and then stirred for 20 min. The homogenate was divided into two equal parts (5 mL × 2), followed by centrifugation. The resulting pellets were homogenized with 5 mL of TBS, 1% Triton X-100 or TBS, 1% Triton X-100, 0.1 M lactose, followed by centrifugation. The resulting pellets (Figure 5A, P4 and P4·Lac) were individually dissolved in 500 μL of 1X SDS sample buffer. This procedure is schematically shown in Figure 5A. The amount of internalized G9Null was estimated by quantitative

western blot analysis: about 25% of G9Null added to the medium was internalized after 16-h culture.

Immunofluorescence microscopy

For immunofluorescence confocal microscopy, PC-3 cells suspended in DMEM-2% FBS at a cell density of 1×10^5 cells/0.45 mL were seeded onto 35-mm glass bottom cell culture dishes (CELLview cell culture dishes with glass bottoms, four compartments; Greiner Bio-One, Frickenhausen, Germany) (0.45 mL/compartment) and then cultured for 24 h. After adding samples (50 μL/compartment), cell cultures were continued for appropriate lengths of time. After removing the medium, cells were washed with PBS. In order to visualize internalized Gal-9, cells were washed twice with PBS, 0.2 M lactose before washing with PBS. The washed cells were fixed with 4% paraformaldehyde in PBS for 20 min at room temperature. A neutralized formaldehyde solution (10%) was used instead of the paraformaldehyde solution for the detection of ubiquitinated proteins. After fixation, cells were treated with 0.25% NH_4Cl in PBS for 10 min to quench aldehyde groups and then permeabilized with 0.1% Triton X-100 in PBS for 10 min prior to incubation with primary antibodies overnight at 4°C. After the incubation with primary antibodies, cells were washed with PBS and then incubated with Alexa Fluor 568-labeled Goat Anti-rabbit IgG (Abcam) and/or fluorescein-labeled antibody to mouse IgG(H + L) (Kirkegaard and Perry Laboratories) for 2 h at room temperature. Cells were washed with PBS before observation by confocal microscopy using an LSM 700 laser scanning confocal microscope (Zeiss, Oberkochen, Germany). For the visualization of actin filaments and nuclei, cells were incubated with FITC-phalloidin (Molecular Probes, Eugene, OR, USA; 1.65×10^{-7} M in PBS, 1 mg/mL BSA) and TO-PRO-3 (Thermo-Fisher Scientific, Waltham, MA USA; ×1/1000 in PBS, 1 mg/mL BSA), respectively, for 20 min after incubation with secondary antibodies.

Lysosomes and autophagosomes in live cells were visualized as follows: PC-3 cells suspended in DMEM-2% FBS at a cell density of 2×10^5 cells/mL were seeded onto 35-mm glass bottom cell culture dishes (0.45 mL/compartment) and then cultured for 24 h. After adding test samples (50 μL/compartment), cells were cultured for appropriate lengths of time. After removing the medium, cells were washed twice with PBS, 2% FBS. The washed cells were incubated with LysoTracker Red DND-99 (Invitrogen, Carlsbad, CA, USA) and CYTO-ID Green Detection Reagent 2 (Enzo Life Sciences, Farmingdale, NY, USA) for 30 min at 37°C. LysoTracker Red DND-99 and CYTO-ID Green Detection Reagent 2 were used at 75 nM and ×1/500 dilution, respectively, in PBS, 2% FBS. After removing the solution, cells were washed with PBS and then Hank's balanced salt solution, 1 mg/mL BSA was added to the compartments. Fluorescence confocal microscopy was carried out with an LSM 700 microscope.

Supplementary data

Supplementary data is available at *Glycobiology* online.

Funding

This study was supported in part by the Ministry of Education, Culture, Sports, Science and Technology, Japan [a Grant-in-Aid for Scientific Research (C), 15K06974 to N.N.].

Conflict of interest statement

None declared.

Abbreviations

CIE, clathrin-independent endocytosis; CME, clathrin-mediated endocytosis; CRC, colorectal cancer; CRD, carbohydrate recognition domain; CSGal-1, a cysteine-less mutant of Gal-1; CSGal-1, a cysteine-less mutant of Gal-1; G9M, a major isoform of wild-type galectin-9; G9Null, a protease-resistant form of galectin-9; GST, glutathione S-transferase; MAPK, mitogen-activated protein kinase.

References

Abramoff MD, Magalhaes PJ, Ram SJ. 2004. Image processing with ImageJ. *Biophotonics Int*. 11:36–42.

Bastiani M, Parton RG. 2010. Caveolae at a glance. *J Cell Sci*. 123: 3831–3836.

Chauhan S, Kumar S, Jain A, Ponpuak M, Mudd MH, Kimura T, Choi SW, Peters R, Mandell M, Bruun JA et al. 2016. TRIMs and galectins globally cooperate and TRIM16 and Galectin-3 Co-direct autophagy in endomembrane damage homeostasis. *Dev Cell*. 39:13–27.

Chou FC, Shieh SJ, Sytwu HK. 2009. Attenuation of Th1 response through galectin-9 and T-cell Ig mucin 3 interaction inhibits autoimmune diabetes in NOD mice. *Eur J Immunol*. 39:2403–2411.

Dikic I, Giordano S. 2003. Negative receptor signalling. *Curr Opin Cell Biol*. 15:128–135.

Dutta D, Donaldson JG. 2012. Search for inhibitors of endocytosis: Intended specificity and unintended consequences. *Cell Logist*. 2:203–208.

Franke TF, Hornik CP, Segev L, Shostak GA, Sugimoto C. 2003. PI3K/Akt and apoptosis: Size matters. *Oncogene*. 22:8983–8998.

Fujita K, Iwama H, Oura K, Tadokoro T, Samukawa E, Sakamoto T, Nomura T, Tani J, Yoneyama H, Morishita A et al. 2017. Cancer therapy due to apoptosis: Galectin-9. *Int J Mol Sci*. 18:74.

He W, Fang Z, Wang F, Wu K, Xu Y, Zhou H, Du D, Gao Y, Zhang WN, Niki T et al. 2009. Galectin-9 significantly prolongs the survival of fully mismatched cardiac allografts in mice. *Transplantation*. 88:782–790.

Hirabayashi J, Kasai K. 1993. The family of metazoan metal-independent beta-galactoside-binding lectins: Structure, function and molecular evolution. *Glycobiology*. 3:297–304.

Hughes RC. 1999. Secretion of the galectin family of mammalian carbohydrate-binding proteins. *Biochim Biophys Acta*. 1473:172–185.

Itoh A, Fukata Y, Miyanaka H, Nonaka Y, Ogawa T, Nakamura T, Nishi N. 2013. Optimization of the inter-domain structure of galectin-9 for recombinant production. *Glycobiology*. 23:920–925.

Johannes L, Parton RG, Bassereau P, Mayor S. 2015. Building endocytic pits without clathrin. *Nat Rev Mol Cell Biol*. 16:311–321.

Kanzaki M, Wada J, Sugiyama K, Nakatsuka A, Teshigawara S, Murakami K, Inoue K, Terami T, Katayama A, Eguchi J et al. 2012. Galectin-9 and T cell immunoglobulin mucin-3 pathway is a therapeutic target for type 1 diabetes. *Endocrinology*. 153:612–620.

Kashio Y, Nakamura K, Abedin MJ, Seki M, Nishi N, Yoshida N, Nakamura T, Hirashima M. 2003. Galectin-9 induces apoptosis through the calcium-calpain-caspase-1 pathway. *J Immunol*. 170:3631–3636.

Katoh S, Ishii N, Nobumoto A, Takeshita K, Dai SY, Shinonaga R, Niki T, Nishi N, Tominaga A, Yamauchi A et al. 2007. Galectin-9 inhibits CD44-hyaluronan interaction and suppresses a murine model of allergic asthma. *Am J Respir Crit Care Med*. 176:27–35.

Kobayashi T, Kuroda J, Ashihara E, Oomizu S, Terui Y, Taniyama A, Adachi S, Takagi T, Yamamoto M, Sasaki N et al. 2010. Galectin-9 exhibits anti-myeloma activity through JNK and p38 MAP kinase pathways. *Leukemia*. 24:843–850.

Komander D, Rape M. 2012. The ubiquitin code. *Annu Rev Biochem*. 81: 203–229.

Kong EH, Kim YJ, Kim YJ, Cho HJ, Yu SN, Kim KY, Chang JH, Ahn SC. 2008. Piplartine induces caspase-mediated apoptosis in PC-3 human prostate cancer cells. *Oncol Rep*. 20:785–792.

Lee J, Lee S, Kim SL, Choi JW, Seo JY, Choi DJ, Park YI. 2014. Corn silk maysin induces apoptotic cell death in PC-3 prostate cancer cells via mitochondria-dependent pathway. *Life Sci*. 119:47–55.

Lu LH, Nakagawa R, Kashio Y, Ito A, Shoji H, Nishi N, Hirashima M, Yamauchi A, Nakamura T. 2007. Characterization of galectin-9-induced death of Jurkat T cells. *J Biochem*. 141:157–172.

Matsumura K, Higashida K, Ishida H, Hata Y, Yamamoto K, Shigeta M, Mizuno-Horikawa Y, Wang X, Miyoshi E, Gu J et al. 2007. Carbohydrate binding specificity of a fucose-specific lectin from Aspergillus oryzae: a novel probe for core fucose. *J Biol Chem*. 282:15700–15708.

Niki T, Tsutsui S, Hirose S, Aradono S, Sugimoto Y, Takeshita K, Nishi N, Hirashima M. 2009. Galectin-9 is a high affinity IgE-binding lectin with anti-allergic effect by blocking IgE-antigen complex formation. *J Biol Chem*. 284:32344–32352.

Nishi N, Abe A, Iwaki J, Yoshida H, Itoh A, Shoji H, Kamitori S, Hirabayashi J, Nakamura T. 2008. Functional and structural bases of a cysteine-less mutant as a long-lasting substitute for galectin-1. *Glycobiology*. 18: 1065–1073.

Nishi N, Itoh A, Fujiyama A, Yoshida N, Araya S, Hirashima M, Shoji H, Nakamura T. 2005. Development of highly stable galectins: Truncation of the linker peptide confers protease-resistance on tandem-repeat type galectins. *FEBS Lett*. 579:2058–2064.

Ohtake F, Tsuchiya H. 2017. The emerging complexity of ubiquitin architecture. *J Biochem*. 161:125–133.

Ohtsubo K, Takamatsu S, Minowa MT, Yoshida A, Takeuchi M, Marth JD. 2005. Dietary and genetic control of glucose transporter 2 glycosylation promotes insulin secretion in suppressing diabetes. *Cell*. 123:1307–1321.

Piper RC, Katzmann DJ. 2007. Biogenesis and function of multivesicular bodies. *Annu Rev Cell Dev Biol*. 23:519–547.

Sakai K, Kawata E, Ashihara E, Nakagawa Y, Yamauchi A, Yao H, Nagao R, Tanaka R, Yokota A, Takeuchi M et al. 2011. Galectin-9 ameliorates acute GVH disease through the induction of T-cell apoptosis. *Eur J Immunol*. 41:67–75.

Seki M, Oomizu S, Sakata KM, Sakata A, Arikawa T, Watanabe K, Ito K, Takeshita K, Niki T, Saita N et al. 2008. Galectin-9 suppresses the generation of Th17, promotes the induction of regulatory T cells, and regulates experimental autoimmune arthritis. *Clin Immunol*. 127:78–88.

Seki M, Sakata KM, Oomizu S, Arikawa T, Sakata A, Ueno M, Nobumoto A, Niki T, Saita N, Ito K et al. 2007. Beneficial effect of galectin 9 on rheumatoid arthritis by induction of apoptosis of synovial fibroblasts. *Arthritis Rheum*. 56:3968–3976.

Takeda K, Noguchi T, Naguro I, Ichijo H. 2008. Apoptosis signal-regulating kinase 1 in stress and immune response. *Annu Rev Pharmacol Toxicol*. 48:199–225.

Thurston TL, Wandel MP, von Muhlinen N, Foeglein A, Randow F. 2012. Galectin 8 targets damaged vesicles for autophagy to defend cells against bacterial invasion. *Nature*. 482:414–418.

Wiersma VR, de Bruyn M, Helfrich W, Bremer E. 2013. Therapeutic potential of Galectin-9 in human disease. *Med Res Rev*. 33:E102–E126.

Wiersma VR, de Bruyn M, Wei Y, van Ginkel RJ, Hirashima M, Niki T, Nishi N, Zhou J, Pouwels SD, Samplonius DF et al. 2015. The epithelial polarity regulator LGALS9/galectin-9 induces fatal frustrated autophagy in KRAS mutant colon carcinoma that depends on elevated basal autophagic flux. *Autophagy*. 11:1373–1388.

Zhu C, Anderson AC, Schubart A, Xiong H, Imitola J, Khoury SJ, Zheng XX, Strom TB, Kuchroo VK. 2005. The Tim-3 ligand galectin-9 negatively regulates T helper type 1 immunity. *Nat Immunol*. 6:1245–1252.